PALEOCEANOGRAPHY, VOL. 28, 740–751, doi:10.1002/2013PA002546, 2013

Time-transgressive North Atlantic productivity changes upon Northern Hemisphere glaciation

K. T. Lawrence,[1] D. M. Sigman,[2] T. D. Herbert,[3] C. A. Riihimaki,[4] C. T. Bolton,[5] A. Martinez-Garcia,[6,7] A. Rosell-Mele,[7,8] and G. H. Haug[6]

Received 1 August 2013; revised 6 November 2013; accepted 18 November 2013; published 23 December 2013.

[1] Marine biological export productivity declined in high-latitude regions in the North Pacific and Southern Ocean 2.7 million years ago, in parallel with the intensification of Northern Hemisphere glaciation. Here we present data from the North Atlantic, which show a similar but time-transgressive pattern of high-latitude productivity decline from 3.3 to 2.5 Ma, with productivity decreasing first at 69°N, hundreds of thousands of years before it declined at 58°N. We propose that the cumulative data are best explained by an equatorward migration of the westerly winds, which caused a southward shift in the zone of Ekman divergence and upwelling-associated major nutrient supply over this time interval. We suggest that a similar equatorward migration of the westerly winds may also help explain the productivity changes observed in other high-latitude regions, particularly the Southern Ocean. At 2.7 Ma, equatorial and temperate Atlantic sites began to show orbitally paced productivity pulses, consistent with a shoaling and meridional contraction of the nutrient-poor "warm sphere" that characterizes the low latitude upper ocean. This timing coincides with observed productivity changes in Southern Ocean, consistent with previous findings that the Southern Ocean exerts a strong influence on the fertility of the low-latitude Atlantic. Finally, we propose that the unique basin geometry of the North Atlantic caused deep water formation in this region to remain relatively stable despite equatorward migration of winds and ocean fronts.

Citation: Lawrence, K. T., D. M. Sigman, T. D. Herbert, C. A. Riihimaki, C. T. Bolton, A. Martinez-Garcia, A. Rosell-Mele, and G. H. Haug (2013), Time-transgressive North Atlantic productivity changes upon Northern Hemisphere glaciation, *Paleoceanography*, *28*, 740–751, doi:10.1002/2013PA002546.

1. Introduction

[2] The intensification of Northern Hemisphere glaciation (NHG) ~2.7 Ma resulted in a wide array of changes in regions both proximal to and far afield from Northern Hemisphere ice sheets [*Haug et al*., 1999; *Jansen et al*., 2000; *Shackleton et al*., 1984; *Sigman et al*., 2004], including an abrupt decline in the sedimentary accumulation of diatom-derived biogenic opal in both the subarctic North Pacific and in the Antarctic Zone of the Southern Ocean at ~2.7 Ma [*Haug et al*., 1999; *Sigman et al*., 2004] (Figures 1a and 1j). These dramatic reductions in opal accumulation imply important changes in high latitude upper-ocean circulation in association with the intensification of NHG. Nitrogen isotope evidence for a decrease in surface nitrate concentration in association with the North Pacific opal "crash" suggests a reduction in nitrate supply, such as would occur if circulation and water column conditions changed so as to reduce the exchange of water between surface waters and the ocean interior [*Haug et al*., 1999, 2005; *Studer et al*., 2012]. Benthic carbon isotope data from the Southern Ocean indicate that southern sourced waters accumulated respiratory carbon at that time, consistent with reduced Antarctic deep water formation [*Hodell and Venz-Curtis*, 2006]. A range of physical causes has been proposed to explain these polar ocean changes [*Hillenbrand and Cortese*, 2006; *Sigman et al*., 2004; *Toggweiler et al*., 2006]. Yet it has proven difficult to test these potential explanations.

[3] *Bolton et al*. [2011] reported evidence that the North Atlantic underwent changes in productivity during NHG that were reminiscent of, and had a similar timing to, productivity changes in the North Pacific and Southern Ocean. Moreover, the observed high-latitude productivity shifts were similar in timing, but opposite in sign, to productivity shifts observed in low- to middle-latitude regions [*Bolton et al*., 2011].

Additional supporting information may be found in the online version of this article.

[1]Department of Geology and Environmental Geosciences, Lafayette College, Easton, Pennsylvania, USA.
[2]Department of Geosciences, Princeton University, Princeton, New Jersey, USA.
[3]Department of Geological Sciences, Brown University, Providence, Rhode Island, USA.
[4]Council on Science and Technology, Princeton University, Princeton, New Jersey, USA.
[5]Departamento de Geologia, Universidad de Oviedo, Oviedo, Spain.
[6]Department of Earth Sciences, Geological Institute, ETH Zürich, Zürich, Switzerland.
[7]Institut de Ciència i Tecnologia Ambientals, Universitat Autònoma de Barcelona, Catalonia, Spain.
[8]Institucio Catalana de Recerca I Estudis Avancats, Barcelona, Spain.

Corresponding author: K. T. Lawrence, Department of Geology and Environmental Geosciences, Lafayette College, Easton, PA 18042, USA. (lawrenck@lafayette.edu)

0883-8305/13/10.1002/2013PA002546

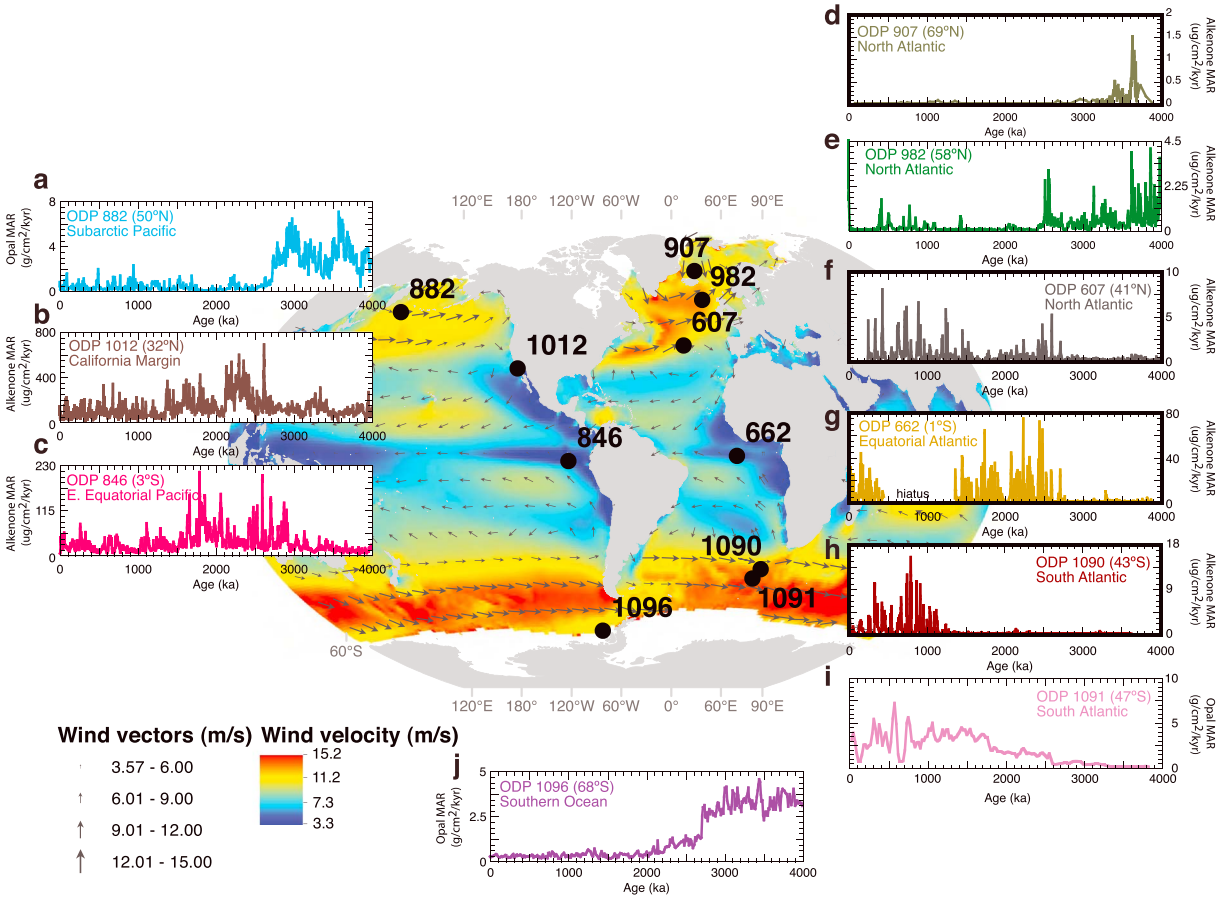

Figure 1. Plio-Pleistocene export productivity synthesis. Locations of sites associated with biogenic opal mass accumulation rate (MAR) (g/cm^2/kyr) or C_{37} alkenone MAR (μg/cm^2/kyr) data shown here. Alkenone data are from sites 907, 607, 662, (this study, highlight by bolded borders), 1090 (this study and [*Martinez-Garcia et al*., 2009], highlighted by bold borders), 846 [*Lawrence et al*., 2006], 982 [*Lawrence et al*., 2009], and 1012 [*Liu et al*., 2008]. Opal data are from sites 882 [*Haug et al*., 1999], 1091 [*Cortese et al*., 2004] and 1096 [*Sigman et al*., 2004]. Site locations are superimposed on a map of modern wind velocities and directions extracted from [*Zhang et al*., 2006a, 2006b].

Accordingly, it was argued that the observed increases in middle- to low-latitude productivity may have been tied to a shoaling of the tropical thermocline as well as physical changes in high southern latitudes that could have increased the nutrient content of sub-Antarctic mode water [*Bolton et al*., 2011], which supplies the waters upwelled in these regions [*Sarmiento et al*., 2004]. Changes in high southern latitudes were attributed to increased sea ice cover, stronger water column stratification and/or a change in the position of the Southern Hemisphere westerly winds. Increased stratification via the transient development of a halocline was offered as the most plausible explanation for the productivity decline observed in the North Atlantic [*Bolton et al*., 2011].

[4] Here we report new paleoproductivity data from a meridional transect of sites in the Atlantic Ocean, which help to discriminate among the various hypotheses previously put forth to explain declines in high-latitude export productivity. The data imply that a southward migration of the westerlies in response to global cooling during the period of early NHG, with its attendant effects on the density stratification of the upper ocean, was the dominant driver of the observed declines in high-latitude North Atlantic productivity. While the evidence is less compelling than in the North Atlantic, previously reported productivity changes in other high-latitude regions [*Haug et al*., 1999; *Sigman et al*., 2004], the Southern Ocean in particular, may also have been driven by the equatorward migration of the westerly wind-driven upwelling. We offer a conceptual model that links these high-latitude physical and biogeochemical changes to similarly timed increases in productivity observed in middle- to low-latitude regions. We also offer a proposal as to how the equatorward migration of winds might give rise to the apparent contrast between Southern Ocean and North Atlantic changes in deep water formation over the Plio-Pleistocene.

2. Materials and Methods

2.1. Proxy Background

[5] We report new proxy records of Plio-Pleistocene ocean productivity based on alkenone concentration data from a transect of Ocean Drilling Program (ODP) sites in the North Atlantic Ocean (sites 907, 607, 662, and 1090) ranging from 69°N to 43°S (Table 1 and Figures 1d, 1f–1h). For new productivity data sets reported here, we used an internal

Table 1. Proxy Records of Plio-Pleistocene Ocean Productivity Atlantic Ocean

SITE	Latitude	Longitude	Water Depth (m)	Paleoproductivity Proxy	Stratigraphic Method	Age Model Citation	Productivity Data Citation
607	41°N	33°W	3427	alkenone MAR	oxygen isotope stratigraphy	*Lisiecki and Raymo*, 2005	this study
662	1°S	12°W	3824	alkenone MAR; biogenic opal MAR	oxygen isotope stratigraphy	*Lisiecki and Raymo*, 2005; *Cleaveland and Herbert*, 2007; *Herbert et al.*, 2010	this study
846	3°S	91°W	3296	alkenone MAR	oxygen isotope stratigraphy	*Lisiecki and Raymo*, 2005	*Liu and Herbert*, 2004; *Lawrence et al.*, 2006
882	50°N	168°E	3244	biogenic opal MAR	magnetostratigraphy; [a]	*Haug et al.*, 1999	*Haug et al.*, 1999
907	69°N	13°W	1801	alkenone MAR; biogenic opal MAR	magnetostratigraphy	*Jansen et al.*, 2000	this study
982	58 N	16°W	1134	alkenone MAR	oxygen isotope stratigraphy [b]	*Lisiecki and Raymo*, 2005	*Bolton et al.*, 2011
1012	32°N	118°W	1772	alkenone MAR	oxygen isotope stratigraphy, [b]	*Brierley et al.*, 2009	*Liu et al.*, 2008
1090	43°S	9°E	3700	alkenone MAR	oxygen isotope stratigraphy; biostratigraphy	*Martinez-Garcia et al.*, 2009, 2010	this study; *Martinez-Garcia et al.*, 2009
1091	47°S	6°E	4363	biogenic opal MAR	magnetostratigraphy; biostratigraphy	*Cortese et al.*, 2004	*Cortese et al.*, 2004
1096	68°S	77°W	3853	biogenic opal MAR	magnetostratigraphy	*Hillenbrand et al.*, 2001	*Sigman et al.*, 2004

[a] Tuning GRAPE to orbital precession.
[b] Correlation to SST data.

reference standard to estimate the total concentration of C_{37} alkenones (mass/grams dry sediment) in each sample. Replicate extractions of a laboratory standard indicate an analytical error of ≤ 10% for these estimates. We calculated mass accumulation rates of alkenones (Alkenone MAR) ($\mu g\,cm^{-2}\ kyr^{-1}$) using C_{37} alkenone concentration data ($\mu g\,g^{-1}$), sedimentation rates ($cm\ kyr^{-1}$), and shipboard estimates of dry bulk density ($g\,cm^{-3}$). The broad patterns of productivity change reported here are maintained when records are displayed as MAR and concentration data (See representative examples Figures S1 and S2 in the supporting information). Previous work indicates strong correlation between alkenone MAR and other indices of past production [*Budziak et al*., 2000; *Rostek et al*., 1997; *Villanueva et al*., 1997, 1998]. Here we treat both biogenic opal and alkenone MAR (Figure 1) as proxies for export productivity. Comparison of these proxies at sites where companion records exist (Figures S1a and S2) as well as previous interproxy comparison studies [*Bolton et al*., 2010, 2011] indicate that these indices are consistent and reasonable estimates of export productivity.

2.2. Age Models

[6] Age models for previously published productivity data sets (sites 846, 882, 982, 1012, 1090, 1091, and 1096) are presented as reported in the initial publications of these data (Table 1). Age models for new data sets reported here (sites 607, 662, 907, and 1090) are all based on site-specific oxygen isotope stratigraphy [*Herbert et al*., 2010; *Lawrence et al*., 2010; *Martinez-Garcia et al*., 2009, 2010], with the exception of ODP site 907, whose age model is primarily based on magnetostratigraphy [*Jansen et al*., 2000] (Table 1). Oxygen isotope stratigraphy for the sites we present novel data from is based upon correlations to the LR04 benthic oxygen isotope stack [*Lisiecki and Raymo*, 2005]. Note that productivity data for site 1090 from 0 to 1.1 Ma were previously published [*Martinez-Garcia et al*., 2009]. The novel data from site 1090 reported here are those from before 1.1 Ma (Figure 1h).

[7] Despite age model uncertainties at site 907 that are due to the reliance of this age model solely on magnetostratigraphy, the difference in timing of productivity crashes at North Atlantic sites 907 and 982 is a robust result. The location of the Matuyama/Gauss (M/G) magnetic reversal (2.58 Ma) in cores at ODP sites 907 and 982 confirms that the North Atlantic productivity crash was time transgressive, occurring first at the more northerly site 907. The productivity crash at site 907 occurs at ~65 m (meters composite depth (mcd)), >5 m below the M/G reversal boundary, whereas the productivity crash at site 982 occurs at ~52 m (mcd), >5 m above the M/G reversal boundary [*Shipboard Scientific Party*, 1996a, 1996b].

2.3. Spectral Analysis

[8] Spectral analysis was performed using the Arand software package [*Howell*, 2001]. All time series were resampled to an even spacing of 2 kyr before spectral analysis. Simple spectra were computed using the Spectra program using a full linear detrend, and the autocovariance function with a 0.0044 bandwidth, 600 kyr window, and 50% lags. Evolutionary phases were computed using the Crospec program applying a full linear detrend with a 0.0044 bandwidth, 600 kyr window, 50% lags, and a sample increment of 50. Phases are

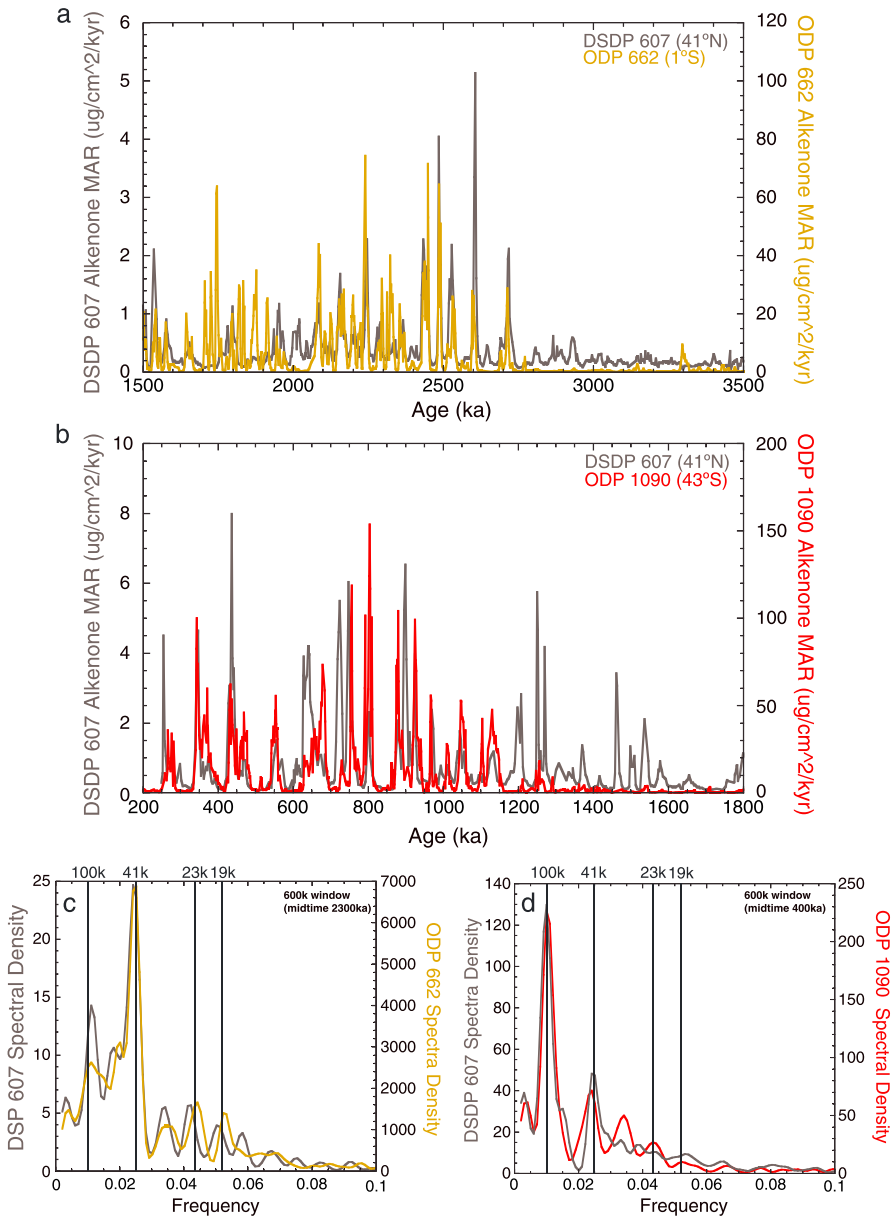

Figure 2. Atlantic Middle to Low Latitude Productivity. (a) C_{37} alkenone MAR (μg/cm^2/kyr) from Site 607 (41°N) (gray) and Site 662 (1°S) (yellow); (b) C_{37} alkenone MAR (μg/cm^2/kyr) from Sites 607 (41°N) (gray) and ODP 1090 (43°S) (red); (c) simple spectra of alkenone MAR data for Site 607 (gray) and 662 (yellow) (window midtime 2300 ka) (d) simple spectra of alkenone MAR for sites 607 (gray) and 1090 (red) (window midtime 400 ka).

reported for intervals that are coherent at the 95% confidence level. We use spectral analysis here to demonstrate that the primary variance in these time series is at orbital frequencies and that the timing of the observed productivity changes, particularly in the dominant frequency band, is similar among the sites we compare. A more complete treatment of the orbital variations in paleoproductivity identified here and the relationship of these variations to other climate variables will be explored in a separate publication.

3. Results

[9] We briefly highlight key features of the data sets reported for the first time here. The high-latitude North Atlantic productivity record at ODP site 907 reveals an abrupt decline in export production at ~3.3 Ma (Figure 1d). In contrast, the middle- to low-latitude productivity data from Atlantic sites 607, 662, and 1090 (Figures 1f–1h) show extremely low productivity during the Pliocene followed by an abrupt rise in orbitally paced productivity peaks starting at 2.7 Ma for sites 607 and 662 (Figures 1f, 1g, and 2a), while productivity pulses begin at site 1090 at 1.25 Ma (Figures 1h and 2b). These middle- to low-latitude records (sites 607, 662, and 1090) demonstrate remarkable structural and spectra similarities (Figure 2). Cross spectral analysis reveals that site 607 and 662 productivity records are highly coherent (0.94) (95% confidence level) and essentially in phase (0.8 kyr ± 2) at the dominant 41 k beat just after productivity

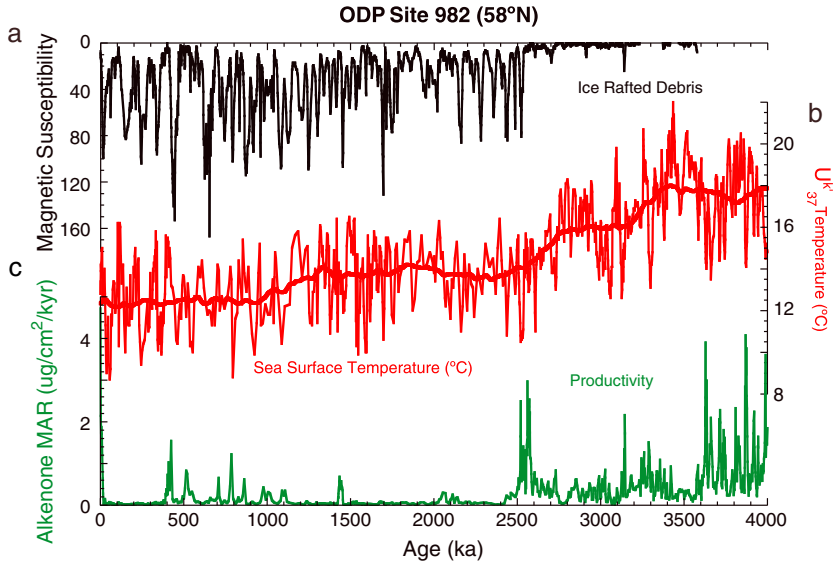

Figure 3. Surface conditions at North Atlantic site 982. (a) Magnetic susceptibility (a proxy for ice-rafted debris) (black) (note inverted axis)[*Shipboard Scientific Party*, 1996a]; (b) $U^{k'}_{37}$ sea surface temperature (°C) estimates (red) [*Lawrence et al*., 2009], and (c) alkenone mass accumulation rates (MAR) (ug/cm^2/kyr) (green) [*Bolton et al*., 2011]. The end of a pronounced cooling step between 3.5 and 2.5 Ma, coincides with a dramatic decrease in productivity at Site 982 and a dramatic increase in ice-rafted debris (IRD).

increases dramatically at both sites (window midtime 2300 ka). Sites 607 and 1090 productivity records are highly coherent at the 100 k (0.99) and 41 k (0.95) orbital beats (95% confidence level) during the latest Pleistocene (window midtime 400 ka). In the 41 k band, these productivity records are also in phase within error (1.5 kyr ± 2), whereas in the 100 k band, site 1090 productivity significantly leads site 607 productivity (18 kyr ± 8).

4. Discussion

4.1. High Latitude Productivity Changes

[10] The high-latitude productivity records in the Northern Hemisphere (sites 907 and 982) [this study; *Bolton et al*., 2011] reveal abrupt Plio-Pleistocene declines in high-latitude North Atlantic productivity analogous to those observed previously in the subarctic North Pacific (site 882) and Antarctic (site 1096) [*Haug et al*., 1999; *Sigman et al*., 2004] (Figures 1a, 1d, 1e, 1j). However, the productivity crashes in the North Atlantic were time transgressive, occurring first at Site 907 (69°N) in the Greenland Sea at ~3.3 Ma and ~800 kyr later at ~2.5 Ma at more southerly Site 982 (58°N) (Figures 1d and 1e). As noted by *Bolton et al*. [2011], the productivity declines evident in both the subarctic North Pacific [*Haug et al*., 1999] (Figure 1a), and North Atlantic (Figures 1d and 1e) coincide with local increases in magnetic susceptibility, a proxy for ice-rafted debris (IRD) (Figure 3a) and IRD concentrations (Figure S1b). Site 607 (41°N), at the southern margin of the modern westerly wind belt, shows the inverse pattern, with low productivity during the early Pliocene and high productivity after 2.7 Ma (Figure 1f). While age model uncertainty is a consideration, opal records from a number of high-latitude sites in the Southern Hemisphere suggest that Southern Ocean changes in productivity roughly mimicked the pattern of progressive equatorward movement of productivity declines observed in the North Atlantic [*Cortese et al*., 2004; *Hillenbrand and Cortese*, 2006].

[11] The similarity between the Pliocene productivity declines observed in the North Atlantic and those from other high-latitude regions in both hemispheres implies a common causal mechanism. Here we make use of the unique features of North Atlantic climate to evaluate the plausibility of each of the mechanisms previously proposed to explain Plio-Pleistocene decreases in high-latitude export productivity. Light limitation driven by ice cover was among the earliest hypotheses for the observed decline in Antarctic productivity since the early Pliocene [*Hillenbrand and Cortese*, 2006]. However, North Atlantic alkenone data indicate temperatures of >8°C (Figure 3b) [*Lawrence et al*., 2009], well above those required for sea ice to have been abundant during the spring-to-summer period of high productivity [*Pflaumann et al*., 2003]. Thus, these high-latitude, North Atlantic data argue instead for a decline in the rate of nutrient supply to polar surface waters as a cause for the observed high-latitude productivity decreases. This conclusion is consistent with previous evidence pointing to reduced nutrient supply as the driver of cooling-related productivity declines in the North Pacific [*Brunelle et al*., 2007; *Haug et al*., 1999; *Jaccard et al*., 2005; *Studer et al*., 2012] and the Antarctic [*Francois et al*., 1997; *Robinson and Sigman*, 2008].

[12] The North Atlantic data also provide constraints on the mechanism behind the decrease in nutrient supply. One proposal to explain a decrease in nutrient supply in the Southern Ocean involves the lower sensitivity of density to temperature at low temperatures, referred to here as the "equation of state" (or "EOS") mechanism [*de Boer et al*., 2007; *Sigman et al*., 2004]. In polar regions, wintertime temperatures are lowest at the surface, encouraging vertical mixing and, in extreme cases, deep water formation; however, the low salinity of polar surface waters works against temperature driven overturning. In the EOS mechanism, global

ocean cooling reduces the effect of temperature on polar ocean density structure, giving the freshness of polar surface waters the upper hand to strengthen density stratification, which discourages vertical mixing and thus reduces nutrient supply to the sunlit surface. However, warm temperatures at North Atlantic site 982 (Figure 3) are problematic for the EOS mechanism. The productivity decline at site 982 occurs at a broadly similar time as in the Antarctic and North Pacific (Figures 1a, 1e, and 1j), and yet the North Atlantic was much warmer than those other two regions at that time, both at the surface (Figure 3) and at depth [*Sosdian and Rosenthal*, 2009]. It appears arbitrary to call upon a more or less coincident EOS-driven increase in upper ocean stratification in regions with such different temperature profiles. Furthermore, North Atlantic $\delta^{13}C$ data from a variety of sites show that North Atlantic overturning persisted in some regions across the Plio-Pleistocene climate transition [*Hodell and Venz-Curtis*, 2006; *Raymo et al*., 1992], indicating that the North Atlantic productivity decline does not represent a North Atlantic-wide end to deep overturning. Therefore, while our data do not preclude a role for the EOS mechanism in reducing Antarctic and North Pacific productivity after ~2.7 Ma, this mechanism now appears poorly suited to provide a blanket explanation for all of the observed high-latitude productivity declines.

4.2. A North Atlantic Westerly Wind Shift

[13] A progressive equatorward migration of North Atlantic climate belts during the late Pliocene has been previously documented by a number of faunal assemblage studies [*Cifelli and Glacon*, 1979; *Dowsett et al*., 1996; *Lutz*, 2011; *Thunell and Belyea*, 1982]. While the zonal mean position of the westerlies is within the midlatitudes, the zonal belt influenced by westerly wind stress is spread across a wider range of latitudes and in the modern lies just equatorward of the most poleward sites included in this synthesis (Figure 1). Thus, we argue that an equatorward shift in the westerlies is the most plausible driver of the time-transgressive Plio-Pleistocene productivity changes observed in the North Atlantic.

[14] Given the smooth nature of spatial gradients in mean atmospheric conditions, Ekman upwelling does not have sharp boundaries, especially at its more polar limit. Thus, Ekman upwelling changes alone may not fully explain the abrupt and dramatic nature of the productivity declines observed in the North Atlantic and elsewhere. Changes in Ekman upwelling also affect the nutrient supply through a feedback on the depth of wintertime mixing. Model studies of wind changes show this dynamic: As local Ekman overturning declines in a given region, the halocline that naturally develops in polar regions due to excess precipitation is no longer so strongly eroded by upwelling from below, and the stronger halocline in turn reduces the depth of winter mixing [*de Boer et al*., 2008]. Thus, we propose that the North Atlantic halocline migrated equatorward over the Plio-Pleistocene, shadowing the poleward edge of the westerlies and causing further reductions in nutrient supply and productivity as the wind migrated out of the region of interest. This proposal is supported by the coincidence of the productivity declines at Sites 907 and 982 with sharp rises in ice rafted debris (Figures 3 and S1b). With a stronger halocline and less vertical mixing, the winter surface layer would have been far more conducive to the survival of drifting sea ice and debris-bearing ice bergs. In this view, the westerly winds drove local climatic and oceanographic changes, with upper ocean density stratification responding to the wind changes. In turn, the strong meridional gradient in atmospheric temperature that would have coincided with the transition into more strongly stratified polar waters may have fed back positively on the equatorward wind shift.

[15] A Northern Hemisphere wind shift is further supported by the relationship between orbitally paced variations in sea surface temperature (SST) and productivity at site 982 before and after its ~2.5 Ma productivity crash (Figure 4). Prior to 2.5 Ma, SSTs were generally warm, and productivity increased in synchrony with shifts toward colder temperatures (glacial conditions) (Figure 4a). In this pre-2.5 Ma regime, we infer that during interglacial times, the core of the westerly winds and Ekman driven surface divergence were slightly north of Site 982. During glacial intervals within this time period, southward migration of the westerly winds brought the zone of strongest Ekman upwelling directly overhead, yielding local productivity maxima. In contrast, after the productivity crash at ~2.5 Ma, the infrequent productivity maxima tended to occur not during peak glacial conditions but rather during deglacial and interglacial intervals (Figure 4b). This change in the productivity-SST relationship suggests that equatorward migration of the westerlies driven by progressive high-latitude cooling (Figure 3) eventually pushed the zone of greatest surface divergence south of Site 982, inhibiting nutrient availability in the surface ocean and leading to the extremely low productivity that characterizes most of this interval (Figures 1e and 4b). The infrequent but notable deglacial increases in productivity observed during this postcrash regime (Figure 4b) are then explained as times when the westerly wind belt and the zone of upwelling were shifted back northward toward and occasionally past Site 982.

4.3. A Bihemispheric Shift in the Westerly Winds?

[16] A prominent hypothesis to drive reduced surface-deep water exchange in the Antarctic of the Last Glacial Maximum involves an equatorward migration of the Southern Hemisphere westerly winds [*Toggweiler et al*., 2006]. The southern westerlies transport polar surface waters equatorward, forming a divergence that draws up deep water into the Antarctic surface layer. According to this hypothesis, if the southern westerly wind belt moved equatorward, it would have begun to move out of the uninterrupted channel of the Southern Ocean, and the surface waters transported northward out of the Antarctic could begin to be replaced by surface waters moving poleward along continental margins, reducing the upwelling of deep water. In addition, the winds may have weakened because of contact with the continents decreasing the upwelling rate. As described above for the North Atlantic, an equatorward shift and/or weakening of the southern westerly winds would have weakened the upwelling of deep water into the Antarctic surface, allowing the Antarctic halocline to strengthen [*de Boer et al*., 2008]. This would have reduced the supply of nutrients to the Antarctic surface and weakened the potential for deep water formation in the Southern Ocean.

[17] Late Pliocene changes in the Southern Ocean productivity records do not, as yet, clearly reveal the time-transgressive pattern recognized in the North Atlantic, but the anticorrelated behavior of polar and subpolar records is apparent, with

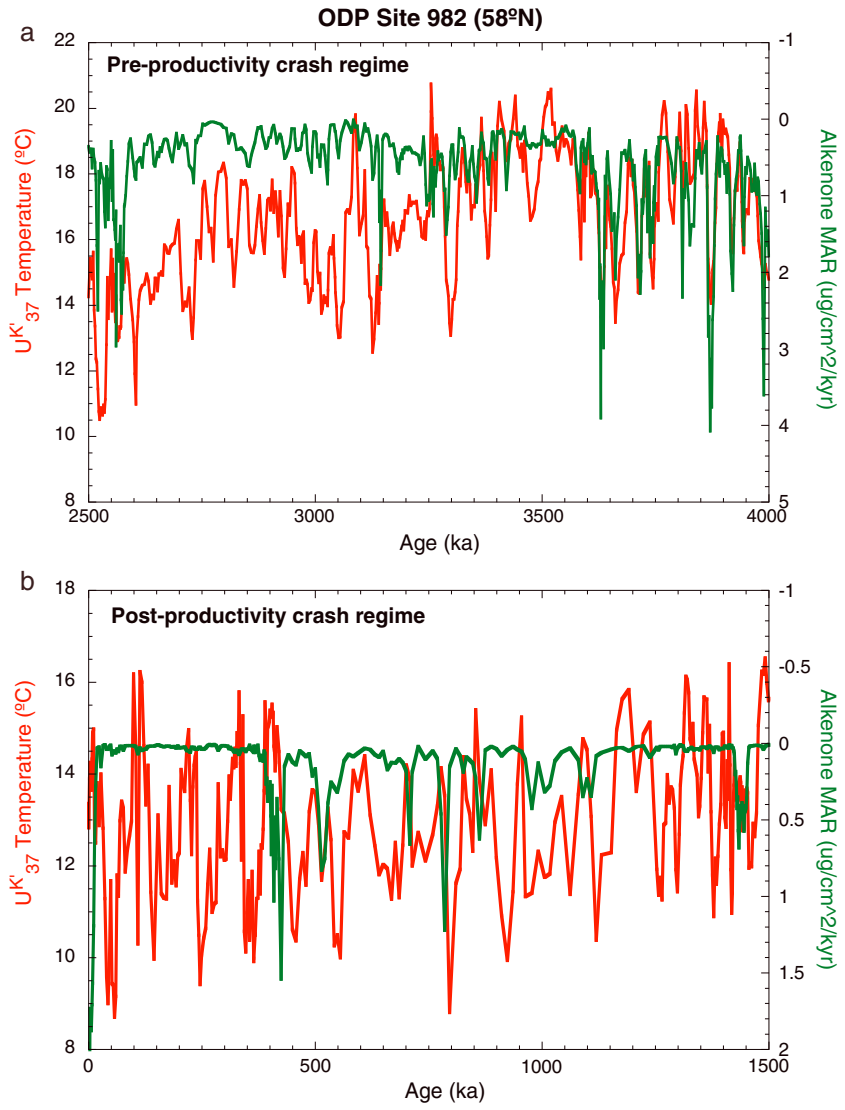

Figure 4. ODP site 982 Surface Conditions. North Atlantic sea surface temperature (red) [*Lawrence et al*., 2009] and C_{37} alkenone MAR (μg/cm^2/kyr) data (green) [*Bolton et al*., 2011] from ODP site 982 (58°N, 16°W) for: (a) preproductivity crash regime (4 to 2.5 Ma) and (b) postproductivity crash regime (1.5 to 0 Ma). Note the axis is inverted for the C_{37} alkenone MAR data.

productivity falling in the Antarctic roughly as it rose in the Subantarctic (Figure 1). Given these observations, we suggest that a bihemispheric equatorward shift in the westerly winds may account for the similar productivity declines observed in northern and southern high latitude regions. The impact of westerly wind shifts on the locus of Ekman divergence provides a simple mechanism for causing similar productivity shifts in high-latitude regions that share little else in common without the requirement that water columns in all of these regions converge toward a similar set of physical conditions at roughly the same time. Additionally, this mechanism is in keeping with the cooling that occurred in high latitudes of both hemispheres during the intensification of NHG. While there is currently much interest in the capacity of eddy transport to weaken the response of upwelling to changes in the westerly winds [e.g., *Marshall and Speer*, 2012], there is little doubt that the latitude of Ekman upwelling is set by that of the westerly winds, and it is a shift in latitude that is the focus of our proposal.

4.4. Connection to Low-Latitude Productivity

[18] Published productivity data sets from middle- to low-latitude regions in the Pacific and Atlantic basins [*Cortese et al*., 2004; *Dekens et al*., 2007; *Lawrence et al*., 2006; *Liu et al*., 2008; *Marlow et al*., 2000] as well as new records reported here from the Atlantic basin (Sites 607 at 41°N, 662 at 1°S) show a pattern inverse to that observed at high latitudes, with marked increases in productivity occurring in association with NHG (e.g., Figures 1b, 1c, 1f, and 1g). Previous studies link low-latitude productivity changes observed in the Pacific to changes in the nutrient content of high-latitude source waters rather than local changes in wind strength because secular changes in productivity and temperature in these regions are decoupled from each other, an observation that is incongruous with a local wind-field mechanism [*Dekens et al*., 2007; *Lawrence et al*., 2006]. While a progressive equatorward migration of the Northern

Hemisphere westerly winds could have enhanced nutrient supply to midlatitude Site 607 by wind-driven Ekman divergence, this mechanism does not apply to Site 662 on the equator. Yet the synchronicity (0.8 kyr ± 2 kyr, essentially in phase in the dominant 41 kyr band) and structural similarity of productivity changes at 607 and 662 suggest a common driver operating in the Atlantic (Figure 2). In addition, the productivity increases at sites 607, 662 (Figures 1f and 1g), and U1313 (41°N, 33°W) [*Naafs et al*., 2010] coincide with the sharp productivity decline in the Antarctic at 2.7 Ma (Site 1096) (Figure 1j) and a deep Southern Ocean $\delta^{13}C$ decline interpreted to indicate reduced Antarctic deep water formation at that time [*Hodell and Venz-Curtis*, 2006]. Thus, we seek an explanation for pattern observed in these middle- to low-latitude Atlantic productivity records that also involves changes in the Southern Hemisphere.

[19] The nutrient content of the middepth ocean is controlled to a substantial degree by the nutrient concentrations of Subantarctic and Antarctic Polar Frontal surface waters [*Sarmiento et al*., 2004]. An equatorward shift in the Southern Hemisphere westerly winds has been proposed to reduce upwelling in the Antarctic and, in turn, Antarctic deep water formation [*Hodell and Venz-Curtis*, 2006]. Such a shift would also likely shift the zone of maximum upwelling equatorward, enhancing Subantarctic productivity while shifting equatorward the surface outcrops of isopycnals and their associated nutrient concentrations. This equatorward shift would yield a basin-wide shoaling of the low-latitude thermocline and a corresponding shoaling of the nutricline (Figure 5). With a shallower nutricline, augmented productivity is to be expected in tropical upwelling zones and at the poleward margin of the North Atlantic gyre (Figure 5). The early response of productivity at sites in the Pacific upwelling regions (e.g., Sites 846 and 1012 at ~3 Ma) relative to the Atlantic (e.g., Sites 607 and 662 at 2.7 Ma) (Figure 1) might be attributable to their connection to deeper isopycnals that are plumbed from higher-latitude surface water in the Southern Ocean, which would have been impacted earlier by a changing Southern Hemisphere wind and nutrient regime.

[20] Our baseline interpretation of the productivity increases at sites 607 and 662 is that the shoaling of the thermocline and contraction of the Atlantic warm pool resulted in nutrient-rich waters at a shallower depth in the water column (Figure 5). Climatically appropriate conditions, as introduced by extrema in the orbital cycles, could then import these nutrients into the low- and middle-latitude mixed layer, driving the productivity pulses (e.g., Figures S3a and S4). In this context, the abrupt onset of these productivity pulses and their lag relative the decline in temperature at these low- and middle-latitude sites might be attributed to the observation from the modern ocean that the nutricline is sharper and deeper than the thermocline. However, one challenge to this interpretation is the synchronous timing of the productivity increases at 662 and 607 (2.7 Ma), which would seem to require that the critical threshold for the outcropping of the nutricline in the surface ocean was reached at both of these sites at exactly the same time.

[21] A potential alternative explanation for the lag between the onset of declining SSTs and of productivity increases, for the coincident initiation of productivity pulses at 662 and 607, and for the greater proportional changes in productivity than in SST on glacial-interglacial timescales at the 2.7 Ma transition is that the nutrient content of individual isopycnals increased as they shoaled [*Lawrence et al*., 2006]. For this to occur, Ekman overturning must transfer more nutrients equatorward than previously, increasing the ratio of equatorward nutrient transport to nutrient uptake by phytoplankton. This might have occurred if the westerly winds strengthened as they migrated equatorward [*Rea et al*., 1998].

[22] If the shoaling and equatorward contraction of the nutrient-poor warm pool explains the increases in productivity at sites 662 (1°S) and 607 (41°N) at ~2.7 Ma (Figures 1f and 1g), then nutrient supply and productivity would also be expected to rise in the subpolar Southern Ocean at about this time. At site 1091 (47°S), the first rise in productivity indeed occurs at ~2.7 Ma (Figure 1i). However, further equatorward at site 1090 (43°S), productivity does not rise until 1.25 Ma (Figure 1h). While sites 607 and 1090 have similar mixed layer densities today, Site 607 may tap significantly deeper isopycnals during ice ages, when the North Atlantic experienced particularly marked cooling (Figure S3a) [*Lawrence et al*., 2010].

[23] Alternatively, the late rise in site 1090 productivity may be related to iron limitation, which plays a key role in producing the high-nutrient, low-chlorophyll conditions of the modern day Southern Ocean [*Blain et al*., 2007]. A reconstruction of Southern Ocean dust-borne iron deposition over the past 4 Ma from ODP site 1090 indicates that aeolian iron supply to the Southern Ocean increased most dramatically around 1.25 Ma [*Martinez-Garcia et al*., 2011], coinciding with the sharp increase in export production at this site (Figure 1h). The productivity increase occurs somewhat later than $\%C_{37:4}$ alkenone (a tracer for the presence of polar waters) rises at ODP site 1090, the latter marking the connection of polar surface waters to Subantarctic surface waters at this time [*Martinez-Garcia et al*., 2010]. These observations suggest that factors beyond circulation and climate may be important for the productivity history of this region. Since site 1090 (at 43°S) is well equatorward of the modern latitudes of Ekman upwelling, it must rely more strongly on dust-driven iron supply (as opposed to upwelled iron) than sites further south (such as site 1091 at 47°S). Therefore, the lateness of the productivity rise at site 1090 may have been due to iron limitation until the dust flux increase at 1.25 Ma [*Martinez-Garcia et al*., 2011].

4.5. Synchronous Orbital Cycles in Subpolar and Equatorial Productivity

[24] Once a new high productivity regime was established in middle- to low-latitude regions in the late Pliocene to earliest Pleistocene, productivity variations occurred at orbital periodicities (Figures 2c and 2d). The strength and coherence of the orbitally driven variations and the synchrony of both the onset of a higher productivity regime and the establishment of a dominant 41 k orbital beat between mid latitude North Atlantic (i.e., Site 607) and tropical Atlantic (i.e., Site 662) paleoproductivity records are remarkable. However, the relationship of these orbitally driven cycles to the secular changes described above is not yet clear. As with the long-term trends, the orbital cycles in productivity may be driven by global cooling, westerly wind shifts in both hemispheres, and the associated contraction of the warm pool, which altered the depth of the nutricline underlying sites 662 and 607. This possibility is consistent with the tight

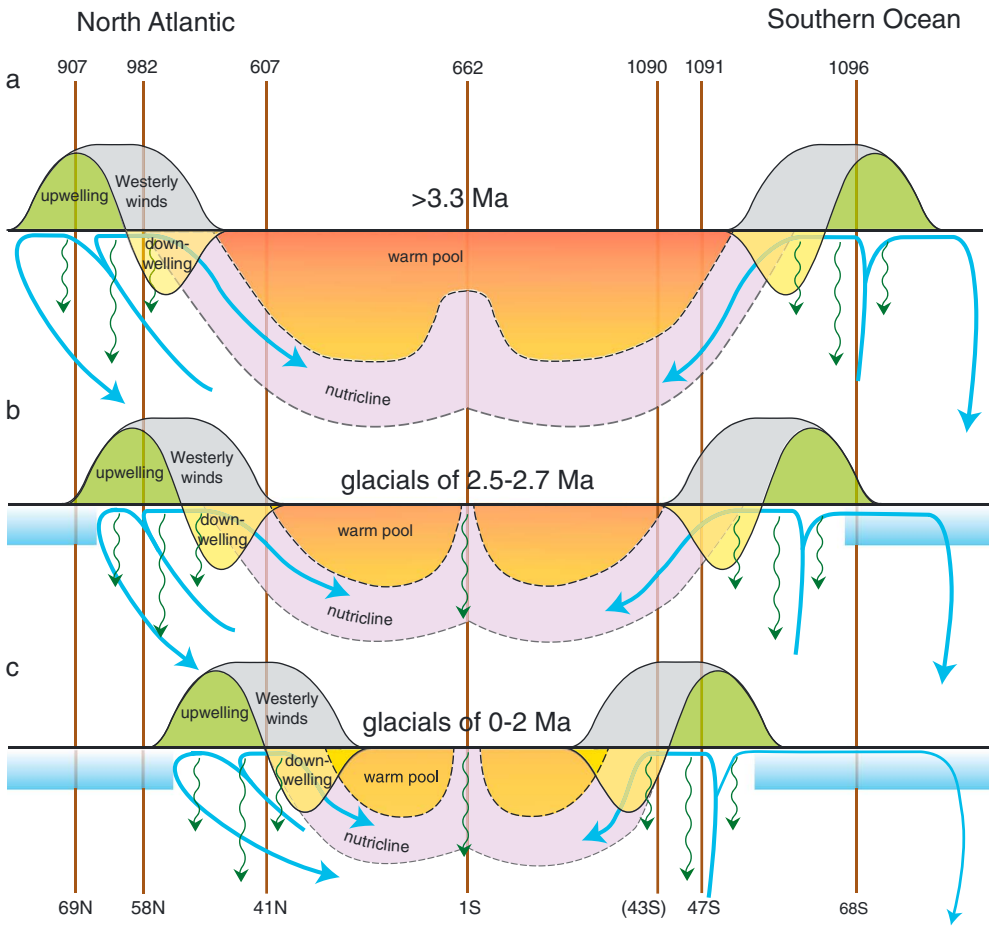

Figure 5. Conceptual Model. A schematic cross section of the Atlantic Ocean illustrating three different productivity regimes during the Plio-Pleistocene. The relative latitudinal positions of site locations from Figure 1 are shown with vertical dark brown lines. Water mass circulation is shown with blue lines and arrows and zones of surface production are indicated with green vertical arrows. (a) Before 3.3 Ma exposure of deep water in polar regions of both hemispheres, limited communication between subsurface and surface in middle- to low-latitude regions. (b) transitional interval (2.5–2.7 Ma), equatorward contraction of warm pools, and migration of westerly wind belts moves productivity equatorward and promotes high-latitude stratification (blue rectangles). (c) ice ages (0–2 Ma), westerly wind belts and associated zones of high productivity are shifted even further equatorward. Deep water production weakens in the Southern Hemisphere and shoals in the Northern Hemisphere as zones of high-latitude stratification expand. Parentheses around site 1090's latitude indicates that the distance between this site and 1091 is exaggerated here.

coupling of SST and productivity at site 607 over orbital cycles (Figure S3). However, other processes may be at work at individual sites, synchronized by changing global climate. For example, glacial strengthening of the trade winds may have played a role in the productivity maxima at site 662, while glacial increases in dust delivery likely enhanced productivity at Subantarctic site 1090 [*Martinez-Garcia et al.*, 2011]. The synchrony among records calls upon a process for "globalizing" the climate changes associated with orbital cycles. Atmospheric CO_2 is a likely globalizer [*Herbert et al.*, 2010], and the southern component of the bihemispheric westerly wind contraction may be central in its orbital variation [*Toggweiler et al.*, 2006]. Thus, the wind shift changes described here may be both a consequence and a cause of orbital and secular climate change; indeed, by this description, they would be a central positive feedback behind Plio-Pleistocene climate change.

5. Conceptual Model

[25] To account for the existing Plio-Pleistocene paleoproductivity observations, we propose the following conceptual model. In the early Pliocene (>3.3 Ma), weaker meridional temperature gradients and a more poleward position of wind belts [*Brierley et al.*, 2009] resulted in the exposure of nutrient-rich deep water in high latitude regions of both hemispheres (Figure 5a). High productivity in these regions contrasts with low-productivity in middle- to low-latitude regions imposed by an expanded warm pool [*Brierley et al.*, 2009] and a deep nutricline. High-latitude cooling during the late Pliocene [*Lawrence et al.*, 2010; *Martinez-Garcia et al.*, 2010] resulted in an equatorward shift of the westerly wind belts in both hemispheres, changing the locus of Ekman divergence and thus the upwelling of deep, nutrient-rich waters into the surface ocean (Figure 5). The progressive movement of the

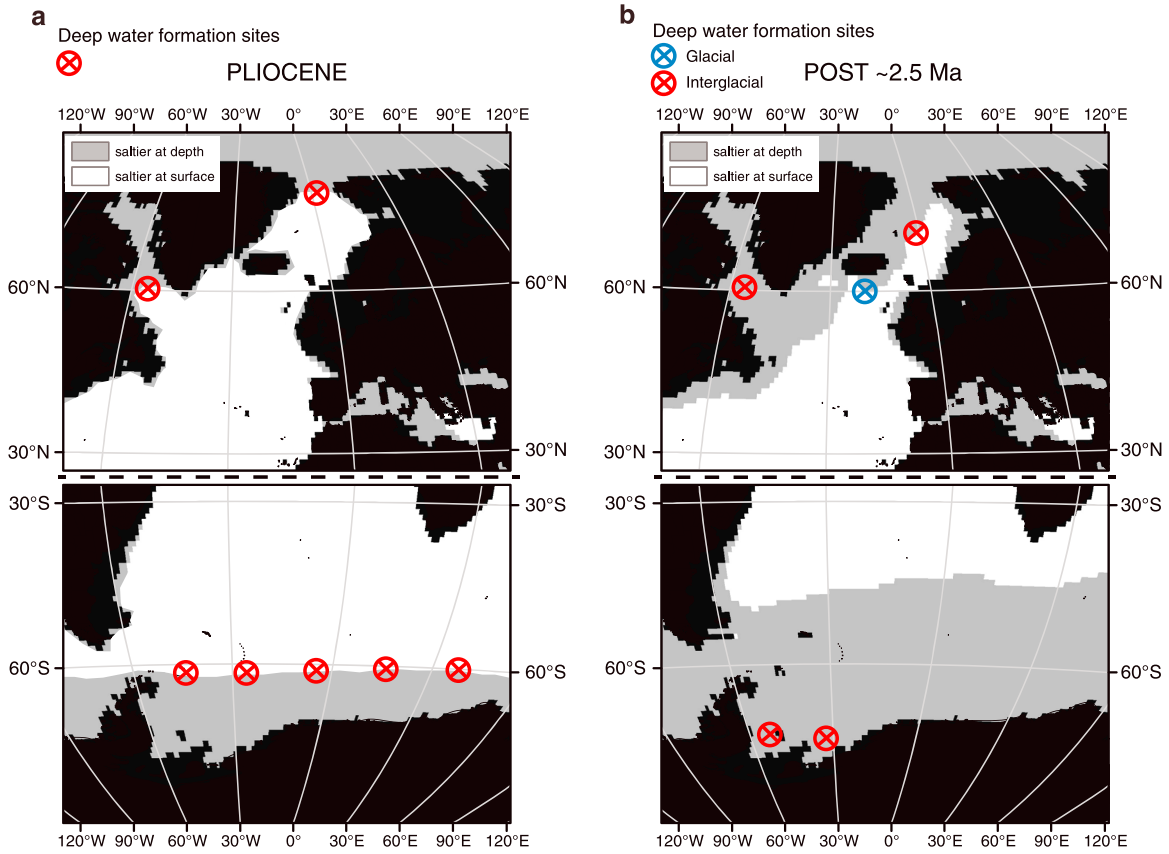

Figure 6. Atlantic upper ocean salinity. (a) Inferred Pliocene pattern; (b) post 2.5 Ma "modern" pattern [*Antonov et al.*, 2010]. Areas shaded gray indicate regions where the water column is saltier at 400–500 meters than at the surface (0–100 m) (i.e., a halocline exists) and areas shaded white indicate regions where the water column is saltier at the surface. Modern and inferred past deepwater formation sites are indicated by Xs, red for warm climate intervals (Pliocene and interglacials of the Pleistocene) and blue for glacial intervals of the Pleistocene.

westerlies away from the poles gave rise to time-transgressive high-latitude productivity crashes in both hemispheres as reduced local Ekman divergence and a resulting increase in density stratification inhibited the mixing of nutrients into the surface ocean in these regions (Figure 5b). The equatorward migration of Ekman divergence not only increased productivity in subpolar regions, but also shoaled the tropical thermocline and nutricline (Figure 5b). The progressive contraction of the warm pool and shoaling of the thermocline and nutricline during the Plio-Pleistocene [*Brierley et al.*, 2009; *Martinez-Garcia et al.*, 2010] (Figures 5b and 5c) gave rise to the increases in productivity observed in lower-latitude regions (Figure 1b, 1c, and 1f–1h).

6. Implications for Deep Water Formation

[26] Because of the importance of global deep water formation for high-latitude climate and atmospheric CO_2, there is an ongoing effort to reconstruct North Atlantic and Southern Ocean ventilation of the ocean interior since the Pliocene. The available data indicate that North Atlantic Deep Water formation was vigorous in the warm mid-Pliocene and did not clearly weaken or strengthen in association with the intensification of Northern Hemisphere glaciation at ~2.7 Ma [*Haug and Tiedemann*, 1998]. In contrast, deep ocean $\delta^{13}C$ data have been interpreted to indicate a sharp reduction in Antarctic-sourced ventilation of the deep ocean at the 2.7 Ma transition [*Hodell and Venz-Curtis*, 2006]. In the context of a hemispherically symmetric ocean, a hemispherically symmetric equatorward migration of the westerlies and oceanographic fronts could not explain a North–South contrast in deep water formation changes. However, we speculate that such an equatorward migration, occurring in the context of the North Atlantic's unique basin configuration, may have contributed to different responses of North Atlantic and Southern Ocean deep ventilation to late Pliocene cooling.

[27] This proposal hinges on the effect of the polar halocline to discourage open ocean deep water formation. In the mid-Pliocene, both northern and southern haloclines would have been restricted to the most polar latitudes (gray shading in Figure 6). Thus, surface waters at high latitudes could have reached relatively cool conditions while Ekman upwelling would have kept their haloclines relatively weak. Under these conditions, it would appear that deep water convection would have been possible in both the North Atlantic and the Southern Ocean (Figure 6a).

[28] With the equatorward migration of the Ekman upwelling regions, the polar haloclines expanded in both hemispheres (gray regions in Figure 6b). We suggest that this change introduced an impediment to Southern Ocean deep water

formation that did not apply to North Atlantic deep water formation. The polar halocline, which works against temperature to stabilize the water column, is adequate to prevent open ocean convection in the modern Southern Ocean and (we infer) previous interglacials since ~2.5 Ma, relegating deep water formation to discrete shelf environments (red Xs in Figure 6b). During recent glacials, even this coastal deep water formation may have been lost (Figure 6b). In the North Atlantic, however, the western continental boundary and zonally thin basin geometry allow the modern North Atlantic Current to pierce the northern polar halocline, carrying salty surface waters into the Greenland and Norwegian Seas, where subsequent cooling allows a salty version of deep water to form (Figure 6b). During the last ice age, even with an apparent equatorward advance in fresh surface waters [*de Vernal et al*., 2002; *Duplessy et al*., 1991] the North Atlantic Current was still able to reach into the region and drive Glacial North Atlantic Intermediate Water formation. Thus, while Antarctic deep water formation may have been inhibited or prevented by the extent of the polar halocline over the Plio-Pleistocene, North Atlantic overturning was likely insensitive to this effect, responding simply by moving deep water formation equatorward as cooling proceeded.

[29] We do not argue that this North/South bias is a full explanation for the decline in Antarctic deep water formation at the 2.7 Ma transition [*Hodell and Venz-Curtis*, 2006]. We have assumed above that the westerlies migration over the Pliocene occurred in response to climate cooling. This implies that Pliocene ocean surface regions that were equatorward of the polar haloclines were also warmer than they were after equatorward migration of the westerlies. Given the relatively weak warming of the tropics during the Pliocene [*Fedorov et al*., 2013] this implies that the halocline-free subpolar regions of the mid-Pliocene would have had SSTs that were more similar to tropical SST during this time. Thus, the lack of a halocline would have been at least partly offset by a relatively higher SST in determining whether deep water could form in the subpolar to polar Southern Ocean during the mid-Pliocene.

[30] Rather, the point we wish to emphasize is that the geometry of the North Atlantic basin may have helped to maintain deep water formation under various climate states, and this may be fundamental to interbasin differences in Plio-Pleistocene deep water formation changes. North Atlantic-sourced deep water has a low preformed nutrient content, such that greater proportional ventilation of the ocean by the North Atlantic translates to a stronger global ocean biological pump and thus lower atmospheric CO_2 [*Hain et al*., 2011; *Marinov et al*., 2008; *Sigman et al*., 2010]. Therefore, the maintenance of North Atlantic deep water formation in the face of reduced Southern Ocean ventilation of the deep ocean may help to explain the apparent Plio-Pleistocene CO_2 decline [*Seki et al*., 2010].

[31] **Acknowledgments.** We acknowledge the Ocean Drilling Program for providing sediment samples. This work was supported by National Science Foundation grants OCE0623310 (K.T.L.), OCE0447570 (D.M.S.), OCE0623487 (T.D.H.), and Spanish Ministry of Science and Innovation grant AP2004-7151 (A.M.G.). We thank H. White, L.C. Peterson, A. Alpert, J. Morabito, A. Mulligan, C. Brown, D. Murray, A. Martin, S. Clemens, A. Tzanova, and W. McClees for their contributions to this work.

References

Antonov, J. I., D. Seidov, T. P. Boyer, R. A. Locarnini, A. V. Mishonov, H. E. Garcia, O. K. Baranova, M. M. Zweng, and D. R. Johnson (2010), in *World Ocean Atlas 2009*, Salinity, NOAA Atlas NESDIS 69, vol. 2, edited by S. Levitus, pp. 184, U.S. Government Printing Office, Washington, D. C.

Blain, S., et al. (2007), Effect of natural iron fertilization on carbon sequestration in the Southern Ocean, *Nature*, *446*(7139), 1070–1074.

Bolton, C. T., K. T. Lawrence, S. J. Gibbs, P. A. Wilson, L. C. Cleaveland, and T. D. Herbert (2010), Glacial-interglacial productivity changes recorded by alkenones and microfossils in the late Pliocene eastern equatorial Pacific and Atlantic upwelling zones, *Earth Planet. Sci. Lett.*, *295*, 401–411.

Bolton, C. T., K. T. Lawrence, S. J. Gibbs, P. A. Wilson, and T. D. Herbert (2011), Biotic and geochemical evidence for a global latitudinal shift in ocean biogeochemistry and export productivity during the late Pliocene, *Earth Planet. Sci. Lett.*, *308*, 200–210.

Brierley, C. M., A. V. Fedorov, Z. Liu, T. D. Herbert, K. T. Lawrence, and J. P. LaRiviere (2009), Greatly expanded tropical warm pool and weakened hadley circulation in the early Pliocene, *Science*, *323*, 1714–1718.

Brunelle, B. G., D. M. Sigman, M. S. Cook, L. D. Keigwin, G. H. Haug, B. Plessen, G. Schettler, and S. L. Jaccard (2007), Evidence from diatom-bound nitrogen isotopes for subarctic Pacific stratification during the last ice age and a link to North Pacific denitrification changes, *Paleoceanography*, *22*, PA1215, doi:10.1029/2005PA001205.

Budziak, D., R. R. Schneider, F. Rostek, P. J. Muller, E. Bard, and G. Wefer (2000), Late Quaternary insolation forcing on total organic carbon and C-37 alkenone variations in the Arabian Sea, *Paleoceanography*, *15*(3), 307–321.

Cifelli, R., and G. Glacon (1979), New late miocene and Pliocene occurrences of globortalia species from the North Atlantic; and a Paleogeographic review, *J. Foraminiferal Res.*, *9*(3), 210–227.

Cleaveland, L. C., and T. D. Herbert (2007), Coherent obliquity band and heterogeneous precession band responses in early Pleistocene tropical sea surface temperatures, *Paleoceanography*, *22*(PA2216), doi:10.1029/2006PA001370.

Cortese, G., R. Gersonde, C.-D. Hillenbrand, and G. Kuhn (2004), Opal sedimentation shifts in the World Ocean over the last 15 Myr, *Earth Planet. Sci. Lett.*, *224*, 509–527.

de Boer, A. M., D. M. Sigman, J. R. Toggweiler, and J. L. Russell (2007), Effect of global ocean temperature change on deep ocean ventilation, *Paleoceanography*, *22*, PA2210, doi:10.1029/2005PA001242.

de Boer, A. M., J. R. Toggweiler, and D. M. Sigman (2008), Atlantic dominance of the meridional overturning circulation, *J. Phys. Oceanogr.*, *38*(2), 435–450.

de Vernal, A., C. Hillaire-Marcel, W. Peltier, and A. Weaver (2002), Structure of the upper water column in the northwest North Atlantic: Modern versus last glacial maximum conditions, *Paleoceanography*, *17*(4), 1050, doi:10.1029/2001PA000665.

Dekens, P. S., A. C. Ravelo, and M. D. Mc Carthy (2007), Warm upwelling regions in the Pliocene warm period, *Paleoceanography*, *22*, PA3211, doi:10.1029/2006PA001394.

Dowsett, H. J., J. Barron, and R. Poore (1996), Middle Pliocene sea surface temperatures: A global reconstruction, *Mar. Micropaleontol.*, *27*, 13–25.

Duplessy, J. C., L. Labeyrie, A. Juillet-Leclerc, F. Maitre, J. Duprat, and M. Sarnthein (1991), Surface salinity reconstruction of the North Atlantic Ocean during the last glacial maximum, *Oceanol. Acta*, *14*(4), 311–324.

Fedorov, A. V., C. M. Brierley, K. T. Lawrence, Z. Liu, P. Dekens, and A. C. Ravelo (2013), Patterns and mechanisms of early Pliocene warmth, *Nature*, *496*, 43–49.

Francois, R., M. A. Altabet, E. F. Yu, D. M. Sigman, M. P. Bacon, M. Frank, G. Bohrmann, G. Barelle, and L. D. Labeyrie (1997), Contribution of Southern Ocean surface-water stratification to low atmospheric CO_2 concentrations during the last glacial period, *Nature*, *389*(6654), 929–935.

Hain, M. P., D. M. Sigman, and G. Haug (2011), Shortcomings of the isolated abyssal reservoir model for deglacial radiocarbon changes in mid-depth Indo-Pacific Ocean, *Geophys. Res. Lett.*, *38*, L04604, doi:10.1029/2010GL046158.

Haug, G. H., and R. Tiedemann (1998), Effect of the formation of the Isthmus of Panama on Atlantic Ocean thermohaline circulation, *Nature*, *393*, 673–676.

Haug, G. H., D. M. Sigman, R. Tiedemann, T. F. Pedersen, and M. Sarnthein (1999), Onset of permanent stratification in the subarctic Pacific Ocean, *Nature*, *401*(6755), 779–782.

Haug, G. H., et al. (2005), North Pacific seasonality and the glaciation of North America 2.7 million years ago, *Nature*, *433*, 821–825.

Herbert, T. D., L. C. Peterson, K. T. Lawrence, and Z. Liu (2010), Tropical ocean temperatures over the past 3.5 Myr, *Science*, *328*, 1530–1534.

Hillenbrand, C. D., and D. K. Futterer (2001), Neogene to Quaternary deposition of opal on the continental rise west of the Antarctic Peninsula, ODP Leg 178, Sites 1095, 1096, and 1101, in *Proceeding of the Ocean Drilling Program, Scientific Results*, edited by P. F. Barker et al., pp. 1–33, College Station, Texas.

Hillenbrand, C. D., and G. Cortese (2006), Polar stratification: A critical view from the Southern Ocean, *Palaeogeogr. Palaeoclimatol. Palaeoecol.*, *242*, 240–252.

Hodell, D. A., and K. A. Venz-Curtis (2006), Late Neogene history of deepwater ventilation in the Southern Ocean, *Geochem. Geophys. Geosyst.*, *7*, Q09001, doi:10.1029/2005GC001211.

Howell, P. (2001), ARAND time series and spectral analysis package for the Macintosh, Brown University, IGBP PAGES/World Data Center for Paleoclimatology Data Contribution Series 2001–044, NOAA/NGDC Paleocliamtology Program, Boulder, Colorado.

Jaccard, S. L., G. H. Haug, D. M. Sigman, T. F. Pedersen, H. R. Thierstein, and U. Rohl (2005), Glacial/interglacial changes in subarctic North Pacific stratification, *Science*, *308*(5724), 1003–1006.

Jansen, E., T. Fronval, F. Rack, and J. E. T. Channell (2000), Pliocene-Pleistocene ice rafting history and cyclicity in the Nordic Seas during the last 3.5 Myr, *Paleoceanography*, *15*(6), 709–721.

Lawrence, K. T., Z. Liu, and T. D. Herbert (2006), Evolution of the eastern tropical Pacific through Plio-Pleistocene glaciation, *Science*, *312*, 79–83.

Lawrence, K. T., T. D. Herbert, C. M. Brown, M. E. Raymo, and A. M. Haywood (2009), High-amplitude variations in North Atlantic sea surface temperature during the early Pliocene warm Period, *Paleoceanography*, *24*, PA2218, doi:10.1029/2008PA001669.

Lawrence, K. T., S. Sosdian, H. E. White, and Y. Rosenthal (2010), North Atlantic climate evolution through the Plio-Pleistocene climate transitions, *Earth Planet. Sci. Lett.*, *300*, 329–342.

Lisiecki, L. E., and M. E. Raymo (2005), A Pliocene-Pleistocene stack of 57 globally distributed benthic ∂18O records, *Paleoceanography*, *20*, PA1003, doi:10.1029/2004PA001071.

Liu, Z., and T. D. Herbert (2004), High-latitude influence on the eastern equatorial Pacific climate in the early Pleistocene epoch, *Nature*, *427*, 720–723.

Liu, Z., M. A. Altabet, and T. D. Herbert (2008), Plio-Pleistocene denitrification in the eastern tropical North Pacific: Intensification at 2.1 Ma, *Geochem. Geophys. Geosyst.*, *9*, Q11006, doi:10.1029/2008GC002044.

Lutz, B. P. (2011), Shifts in North Atlantic planktic foraminifer biogeography and subtropical circulation during the mid-Piacenzian warm period, *Mar. Micropaleontol.*, *80*, 125–149.

Marinov, I., M. Follows, A. Gnanadesikan, J. L. Sarmiento, and R. D. Slater (2008), How does ocean biology affect atmospheric pCO_2? Theory and models, *J. Geophys. Res.*, *113*, C07032, doi:10.1029/2007JC004598.

Marlow, J. R., C. B. Lange, G. Wefer, and A. Rosell-Mele (2000), Upwelling intensification as part of Pliocene-Pleistocene climate transition, *Science*, *290*, 2288–2291.

Marshall, J., and K. Speer (2012), Closure of the meridional overturning circulation through Southern Ocean upwelling, *Nat. Geosci.*, *5*, 171–180.

Martinez-Garcia, A., A. Rosell-Mele, W. Geibert, R. Gersonde, P. Masque, V. Gaspari, and C. Barbante (2009), Links between iron supply, marine productivity, sea surface temperature, and CO_2 over the last 1.1 Ma, *Paleoceanography*, *24*, PA1207, doi:10.1029/2008PA001657.

Martinez-Garcia, A., A. Rosell- Mele, E. L. McClymont, R. Gersonde, and G. Haug (2010), Subpolar link to the emergence of the modern equatorial Pacific cold tongue, *Science*, *328*, 1550–1553.

Martinez-Garcia, A., A. Rosell-Mele, S. L. Jaccard, W. Geibert, D. M. Sigman, and G. H. Haug (2011), Southern Ocean dust-climate coupling over the past four million years, *Nature*, *476*, 312–316, doi:10.1038/nature10310.

Naafs, B. D. A., R. Stein, J. Hefter, N. Khelifi, S. De Schepper, and G. Haug (2010), Late Pliocene changes in the North Atlantic Current, *Earth Planet. Sci. Lett.*, *298*(3–4), 434–442.

Pflaumann, U., et al. (2003), Glacial North Atlantic: Sea-surface conditions reconstructed by GLAMAP 2000, *Paleoceanography*, *18*(3), 1065, doi:10.1029/2002PA000774.

Raymo, M. E., D. A. Hodell, and E. Jansen (1992), Response of deep ocean circulation to initiation of Northern Hemisphere glaciation (3-2MA), *Paleoceanography*, *7*(5), 645–672.

Rea, D. K., H. Snoeckx, and L. H. Joseph (1998), Late Cenozoic eolian deposition in the North Pacific: Asian drying, Tibetan uplift, and cooling of the northern hemisphere, *Paleoceanography*, *13*(3), 215–224.

Robinson, R. S., and D. M. Sigman (2008), Nitrogen isotopic evidence for a poleward decrease in surface nitrate within the ice age Anarctic, *Quat. Sci. Rev.*, *27*(9–10), 1076–1090.

Rostek, F., E. Bard, L. Beaufort, C. Sonzogni, and G. Ganssen (1997), Sea surface temperature and productivity records for the past 240 kyr in the Arabian Sea, *Deep Sea Res., Part II*, *44*(6–7), 1461–1480.

Sarmiento, J. L., N. Gruber, M. A. Brzezinski, and J. P. Dunne (2004), High-latitude controls of thermocline nutrients and low latitude biological productivity, *Nature*, *427*, 56–60.

Seki, O., G. L. Foster, D. N. Schmidt, A. Mackensen, K. Kawamura, and R. D. Pancost (2010), Alkenone and boron-based Pliocene PCO_2 records, *Earth Planet. Sci. Lett.*, *292*, 201–211.

Shackleton, N. J., et al. (1984), Oxygen isotope calibration on the onset of ice-rafting and history of glaciation in the North Atlantic region, *Nature*, *307*, 620–623.

Shipboard Scientific Party (1996a), Site 982, in *Proceedings of the Ocean Drilling Program, Initial Reports*, edited by E. Jansen et al., pp. 91–138, Ocean Drilling Program, College Station, Texas.

Shipboard Scientific Party (1996b), Site 907 (revisted), in *Proceedings of the Ocean Drilling Program, Initial Results*, edited by E. Jansen, M. E. Raymo, and P. Blum, pp. 223–252 , Ocean Drilling Program, College Station, Texas.

Sigman, D. M., S. L. Jaccard, and G. Haug (2004), Polar ocean stratification in a cold climate, *Nature*, *428*, 59–63.

Sigman, D. M., M. P. Hain, and G. H. Haug (2010), The polar ocean and glacial cycles in atmospheric CO_2 concentration, *Nature*, *466*, 47–55.

Sosdian, S., and Y. Rosenthal (2009), Deep-sea temperature and ice volume changes across the Pliocene-Pleistocene climate transition, *Science*, *325*, 306–310.

Studer, A. S., A. Martinez-Garcia, S. L. Jaccard, F. E. Girault, D. M. Sigman, and G. H. Haug (2012), Enchanced stratification and seasonality in the Subarctic Pacific upon Northern Hemisphere Glaciation - New evidence from diatom-bound nitrogen isotopes, alkenones and archaeal tetraethers, *Earth Planet. Sci. Lett.*, *351–352*, 84–94.

Thunell, R. C., and P. Belyea (1982), Neogene planktonic foraminiferal biogeography of the Atlantic Ocean, *Micropaleontology*, *28*(4), 381–398.

Toggweiler, J. R., J. L. Russell, and S. R. Carson (2006), Midlatitude westerlies, atmospheric CO_2, and climate change during the ice ages, *Paleoceanography*, *31*, PA2005, doi:10.1029/2005PA001154.

Villanueva, J., J. O. Grimalt, E. Cortijo, L. Vidal, and L. Labeyrie (1997), A biomarker approach to the organic matter deposited in the North Atlantic during the last climatic cycle, *Geochim. Cosmochim. Acta*, *61*(21), 4633–4646.

Villanueva, J., J. O. Grimalt, L. D. Labeyrie, E. Cortijo, L. Vidal, and J. Louis-Turon (1998), Precessional forcing of productivity in the North Atlantic Ocean, *Paleoceanography*, *13*(6), 561–571.

Zhang, H.-M., J. J. Bates, and R. W. Reynolds (2006a), Assessment of composite global sampling: Sea surface wind speed, *Geophys. Res. Lett.*, *33*, L17714, doi:10.1029/2006GL02786.

Zhang, H.-M., R. W. Reynolds, and J. J. Bates (2006b), Blended and gridded high resolution global sea surface wind speed and climatology from multiple satellites: 1987–present, American Meteorological Society 2006 Annual Meeting Paper# P2.23, edited, Atlanta Georgia.